Identification and characterization of RBM12 as a novel regulator of fetal hemoglobin expression

Aoi Wakabayashi,[1,2] Maryanne Kihiu,[1] Malini Sharma,[1] A. Josephine Thrasher,[1] Megan S. Saari,[1] Mathieu Quesnel-Vallières,[2,3] Osheiza Abdulmalik,[1] Scott A. Peslak,[1,4] Eugene Khandros,[1] Cheryl A. Keller,[5] Belinda M. Giardine,[5] Yoseph Barash,[2] Ross C. Hardison,[5] Junwei Shi,[6] and Gerd A. Blobel[1]

[1]Division of Hematology, The Children's Hospital of Philadelphia, Philadelphia, PA; [2]Department of Genetics and [3]Department of Biochemistry and Biophysics, Perelman School of Medicine at the University of Pennsylvania, Philadelphia, PA; [4]Division of Hematology/Oncology, Department of Medicine, Hospital of the University of Pennsylvania, Philadelphia, PA; [5]Department of Biochemistry and Molecular Biology, Pennsylvania State University, University Park, PA; and [6]Department of Cancer Biology, Perelman School of Medicine at the University of Pennsylvania, Philadelphia, PA

Key Points

- A CRISPR/Cas9 screen targeting RNA binding proteins identifies RBM12 as a novel HbF regulator.

- RBM12-mediated HbF repression is BCL11A-independent and reliant on its RRM1 domain.

The fetal-to-adult hemoglobin transition is clinically relevant because reactivation of fetal hemoglobin (HbF) significantly reduces morbidity and mortality associated with sickle cell disease (SCD) and β-thalassemia. Most studies on the developmental regulation of the globin genes, including genome-wide genetics screens, have focused on DNA binding proteins, including BCL11A and ZBTB7A/LRF and their cofactors. Our understanding of RNA binding proteins (RBPs) in this process is much more limited. Two RBPs, LIN28B and IGF2BP1, are known posttranscriptional regulators of HbF production, but a global view of RBPs is still lacking. Here, we carried out a CRISPR/Cas9-based screen targeting RBPs harboring RNA methyltransferase and/or RNA recognition motif (RRM) domains and identified RNA binding motif 12 (RBM12) as a novel HbF suppressor. Depletion of RBM12 induced HbF expression and attenuated cell sickling in erythroid cells derived from patients with SCD with minimal detrimental effects on cell maturation. Transcriptome and proteome profiling revealed that RBM12 functions independently of major known HbF regulators. Enhanced cross-linking and immunoprecipitation followed by high-throughput sequencing revealed strong preferential binding of RBM12 to 5′ untranslated regions of transcripts, narrowing down the mechanism of RBM12 action. Notably, we pinpointed the first of 5 RRM domains as essential, and, in conjunction with a linker domain, sufficient for RBM12-mediated HbF regulation. Our characterization of RBM12 as a negative regulator of HbF points to an additional regulatory layer of the fetal-to-adult hemoglobin switch and broadens the pool of potential therapeutic targets for SCD and β-thalassemia.

Introduction

The hemoglobin molecule is a tetramer composed of 2 α- and 2 β-type globin chains. Different isoforms of α- and β-type globin genes are expressed during development, thus changing the composition of hemoglobin. The β-type globin genes comprise 1 embryonic (*HBE*, encoding ε-globin), 2 fetal (*HBG1/2*, encoding γ-globin), and 2 adult (*HBD* and *HBB*, encoding δ- and β-globin, respectively) genes.[1,2] During

late gestation until birth, HBG1/2 are the predominant forms expressed, giving rise to fetal hemoglobin (HbF,$\alpha_2\gamma_2$). After birth, HBG1/2 expression is silenced, whereas the levels of HBB and HBD increase and then remain the primarily expressed β-type globin genes throughout life. The mechanisms controlling this fetal-to-adult switch have been under investigation for decades, with the interest in this process fueled by the recognition that reversal of the switch benefits patients with β-hemoglobinopathies such as sickle cell disease (SCD) and β-thalassemia.[3] Two transcription factors, BCL11A and ZBTB7A/LRF, are the major direct repressors of the HBG1/2 genes in adulthood.[4-6] These factors, along with a host of cofactors, are themselves subject to regulation,[7-9] in some cases via posttranscriptional mechanisms.[10]

Posttranscriptional gene regulation has been implicated in various developmental contexts, including hematopoiesis.[11-16] Posttranscriptional mechanisms diversify the cellular proteome through control of messenger RNA (mRNA) splicing, stabilization, localization, and translation via RNA binding proteins (RBPs).[17] RBPs have been studied in the context of the fetal-to-adult switch. For example, the expression of RBPs LIN28B and IGF2BP1 is developmentally controlled, with predominant expression in fetal erythroid cells followed by silencing in adult cells. Forced expression of either RBP in adult cells markedly induces HBG1/2 production by posttranscriptionally lowering BCL11A levels.[10,18,19] Aside from these examples, our knowledge of RBPs in HbF regulation is sparse. To begin to fill this void, we carried out a CRISPR/Cas9-based genetic screen targeting a collection of RBPs for their ability to alter HBG1/2 levels. We discovered RNA binding motif 12 (RBM12) as a novel repressor of HbF expression. RBM12 is a nuclear RBP that functions in pathways not involving the major known HbF regulators. It binds mRNAs in a selective pattern with a strong bias toward 5′ untranslated regions (UTRs). Remarkably, only 1 of RBM12's 5 RNA recognition motifs (RRMs) is essential for HbF repression, and the addition of a proline-rich linker region to that RRM restores its HbF repressive activity. Thus, RBM12 emerges as a novel HbF repressor, providing an underexplored view into the regulation of the fetal-to-adult hemoglobin switch.

Materials and methods

CRISPR/Cas9 screen

The single guide RNA (sgRNA) library, targeting 341 RBPs, contains a total of 3095 sgRNAs with 3 to 6 sgRNAs per RRM and RNA methyltransferase domain. The library was cloned into the LRG2.1T lentiviral vector, which was used to transduce the human erythroid progenitor cell line HUDEP2 stably expressing spCas9.[20,21] After expansion and differentiation, the top and bottom 10% of HbF-expressing cells were collected via fluorescence-activated cell sorting, and the representation of the sgRNAs enriched in those populations was assessed via sequencing on a MiSeq instrument. Candidates were identified if the ratio of the normalized read counts of sgRNAs in the HbF high vs low populations was ≥1.5 in a majority of the sgRNAs.

Mouse fetal liver cultures

Experiments were approved by the institutional animal care and use committee of the Children's Hospital of Philadelphia (protocol IAC 21-000660). Mouse fetal livers at embryonic day 14.5 were dissected from pregnant wild-type (WT) C57BL/6J females that were crossed with Cas9/Cas9 males. Hematopoietic progenitors were isolated using the EasySep mouse Hematopoietic Progenitor Cell Enrichment Kit (no. 19856; StemCell Technologies). Cells were transduced with retrovirus harboring sgRNAs targeting Rbm12 along with Rosa26 control and selected with 1 μg/mL puromycin for 48 hours in StemPro34 with supplement (no. 10639011; ThermoFisher Scientific). Cells were differentiated for 48 hours and harvested for quantitative reverse transcription polymerase chain reaction (qRT-PCR) and Western blotting.

Sickling assay

Peripheral blood mononuclear cells were isolated using Ficoll-Paque Premium (GE17-5442-02; Sigma) density gradient centrifugation on apheresis waste product collected from deidentified patients with SCD. CD34$^+$ cells were purified via magnetic-assisted cell sorting using ultrapure CD34 Microbeads (MACS CD34$^+$ purification kit; no. 130-100-453; Miltenyi) and magnetic columns (no. 130-042-201; Miltenyi). Cells were differentiated for a total of 21 days, sorted for enucleated RBCs via Hoechst 33342 exclusion, and exposed to 2.5% O$_2$ for 2 hours. Following fixation with 2% glutaraldehyde, sickled cells were quantified manually via bright-field microscopy in a blinded fashion.

eCLIP-seq

Enhanced cross-linking and immunoprecipitation followed by high-throughput sequencing (eCLIP-seq) was performed following the standard operating procedure from ENCODE as described by Van Nostrand et al[22] (details provided in supplemental Materials and Methods). Briefly, RBP-RNA complexes were cross-linked via UV exposure (254 nm, 400 mJ/cm^3), fragmented via RNaseI digestion, and immunoprecipitated with anti-RBM12 antibody (sc-514259; Santa Cruz Biotechnology) coupled to magnetic beads (10003D; ThermoFisher Scientific). Samples were washed, and RNA barcode adapters were ligated, resolved on standard protein gels, and transferred to nitrocellulose membranes. RNA was isolated from a region encompassing 75 kDa above the expected size of the RBP, purified, and reverse-transcribed. Complementary DNA libraries were prepared with Illumina index primers and sequenced on a NextSeq2000 instrument.

RBM12 overexpression

V5 C-terminally tagged RBM12 constructs were rendered conditional via fusion to the estrogen receptor ligand-binding domain (RBM12-ER-V5) and inserted into a lentiviral vector.[4,23] Lentivirus was transduced into HUDEP2 cells, which underwent selection in 10 μg/mL of blasticidin for 4 days. RBM12-ER-V5 was activated by addition of 10 nM 4-hydroxytamoxifen.

Results

A CRISPR/Cas9 screen targeting RPBs identifies novel candidate HbF repressors

To identify RBPs that influence HbF levels, we carried out a CRISPR/Cas9 screen in the adult human erythroblast line HUDEP2,[20,21] targeting 341 RBPs via their RRM and RNA methyltransferase domains (supplemental Figure 1A). The RRM is one category of RNA binding domain that confers binding to target transcripts.[24] Potential HbF repressors were called if a majority of the sgRNAs targeting the RBP were enriched in the HbF high population with HbF activators

enriched in the HbF low population. As expected, the nontargeting (NT) control sgRNAs were evenly distributed among the 2 populations. The sgRNAs against *IGF2BP1* were enriched in the HbF low population, consistent with IGF2BP1's functions as an HbF activator (supplemental Figure 1B).[19] Four RBPs (*SYNCRIP*, *hnRNPM*, *PTBP1*, and *RBM12*) emerged from this screen as potential HbF repressors (Figure 1A). Results were validated by depleting each of these RBPs with 2 independent sgRNAs in HUDEP2 cells. Depletion of each candidate RBP led to a 2- to 4-fold increase in the proportion of erythroid cells expressing HbF, termed F-cells (as measured by flow cytometry), along with a 2- to 4-fold increase in *HBG1/2* mRNA (Figure 1B). Among these, SYNCRIP depletion led to the strongest HbF induction.

RBM12 participates in HbF silencing in primary human erythroid cells

Although the HUDEP2 cell line provides a powerful screening platform, any hits require validation in primary human erythroblasts.

We thus depleted each of the 4 candidate RBPs via CRISPR/Cas9 ribonucleoprotein electroporation of human CD34+ hematopoietic stem and progenitor cells (HSPCs) isolated from 3 healthy donors. As part of a 3-phase erythroid culture system,[25] cells underwent erythroid differentiation for 12 to 15 days prior to analysis. In HUDEP2 cells and CD34+ HSPCs, ≥40% depletion of SYNCRIP, PTBP1, and RBM12 at the protein level was achieved (supplemental Figure 1C). Although hnRNPM protein persisted, the sgRNA cutting efficiency (assayed via Tracking of Indels by DEcomposition, TIDE)[26] was >50% in CD34+ cells, suggesting that the edits resulted in a dysfunctional protein. In contrast to the HUDEP2 validation results, depletion of SYNCRIP increased HbF production only minimally as assayed by flow cytometry, qRT-PCR, and high-performance liquid chromatography (Figure 1C). Loss of PTBP1 or hnRNPM increased HbF levels, but at the cost of cellular maturation and fitness (supplemental Figure 2A-C). Depleting RBM12 induced HbF expression >2-fold at the mRNA and protein levels, along with an increase in the proportion of F-cells.
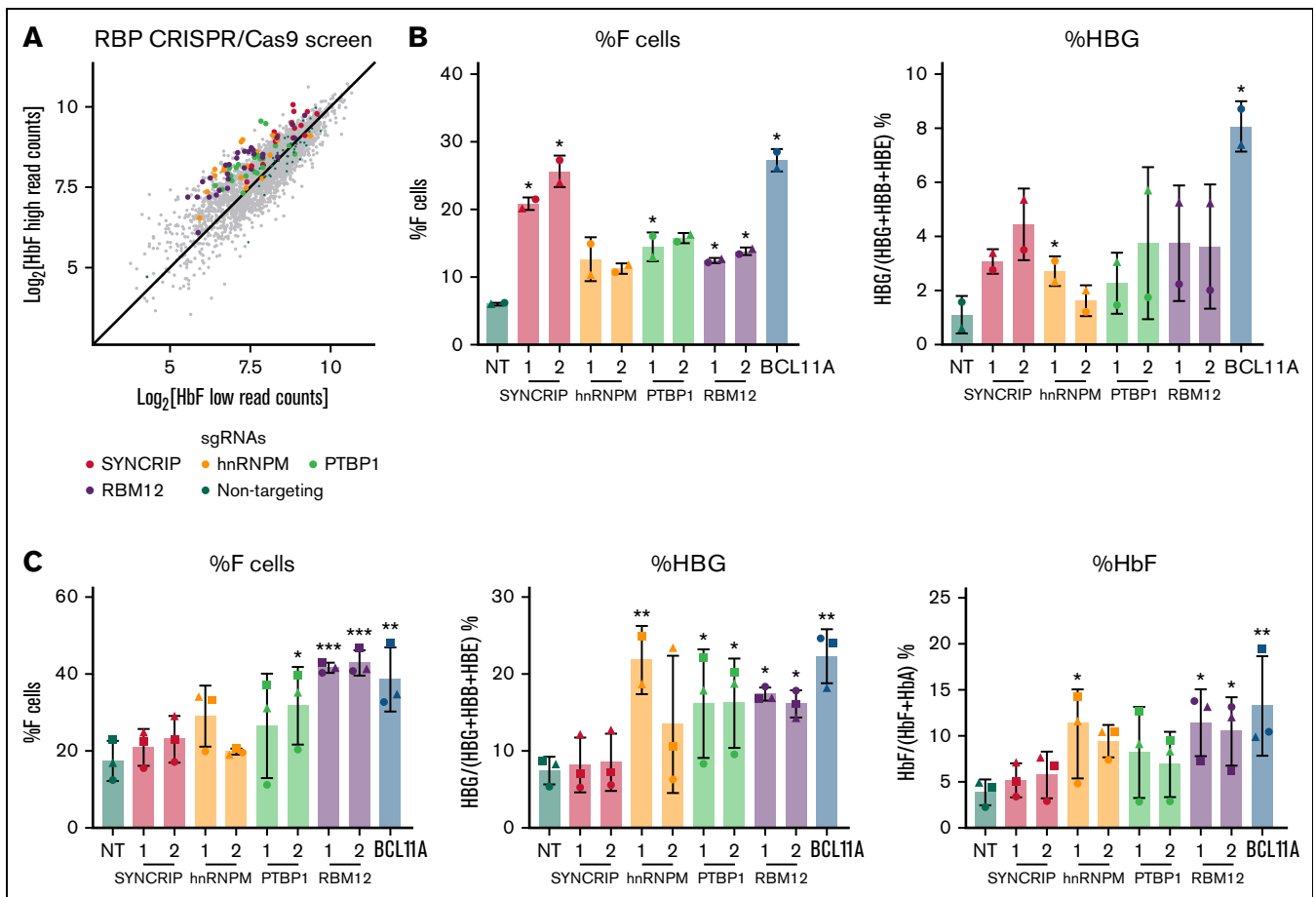

Figure 1. CRISPR/Cas9-based screen identified SYNCRIP, hnRNPM, PTBP1, and RBM12 as candidate HbF regulators. (A) Scatterplot displaying RBP-focused CRISPR/Cas9 screening results. Each dot represents an sgRNA. Highlighted are NT control sgRNAs and sgRNAs targeting candidate HbF regulators. (B) HUDEP2 validation results. Controls are an NT sgRNA and a BCL11A sgRNA targeting exon 2 of BCL11A. Each candidate was targeted with 2 independent sgRNAs (n = 2 biological replicates). Plotted are means ± standard deviation. Left: Percentage of F cells quantified via HbF flow cytometry. Right: qRT-PCR of *HBG1/2* mRNA as percentage of total β-like globin transcripts. Results were normalized to *HPRT1*. *P < .05 by Student's t test. (C) CD34+ HSPC validation result. Controls are NT and a BCL11A sgRNA targeting the +58 erythroid enhancer of BCL11A. Each candidate was targeted with 2 independent sgRNAs (n = 3 biological replicates). Plotted are means ± standard deviation. *P < .05, **P < .01, and ***P < .001 by Student's t test. Left: Percentage of HbF+ cells quantified via HbF flow cytometry. Center: qRT-PCR of *HBG1/2* mRNA as percentage of total β-like globin transcripts. Results were normalized to *HPRT1*. Right: Percentage of HbF relative to NT quantified via high-performance liquid chromatography.
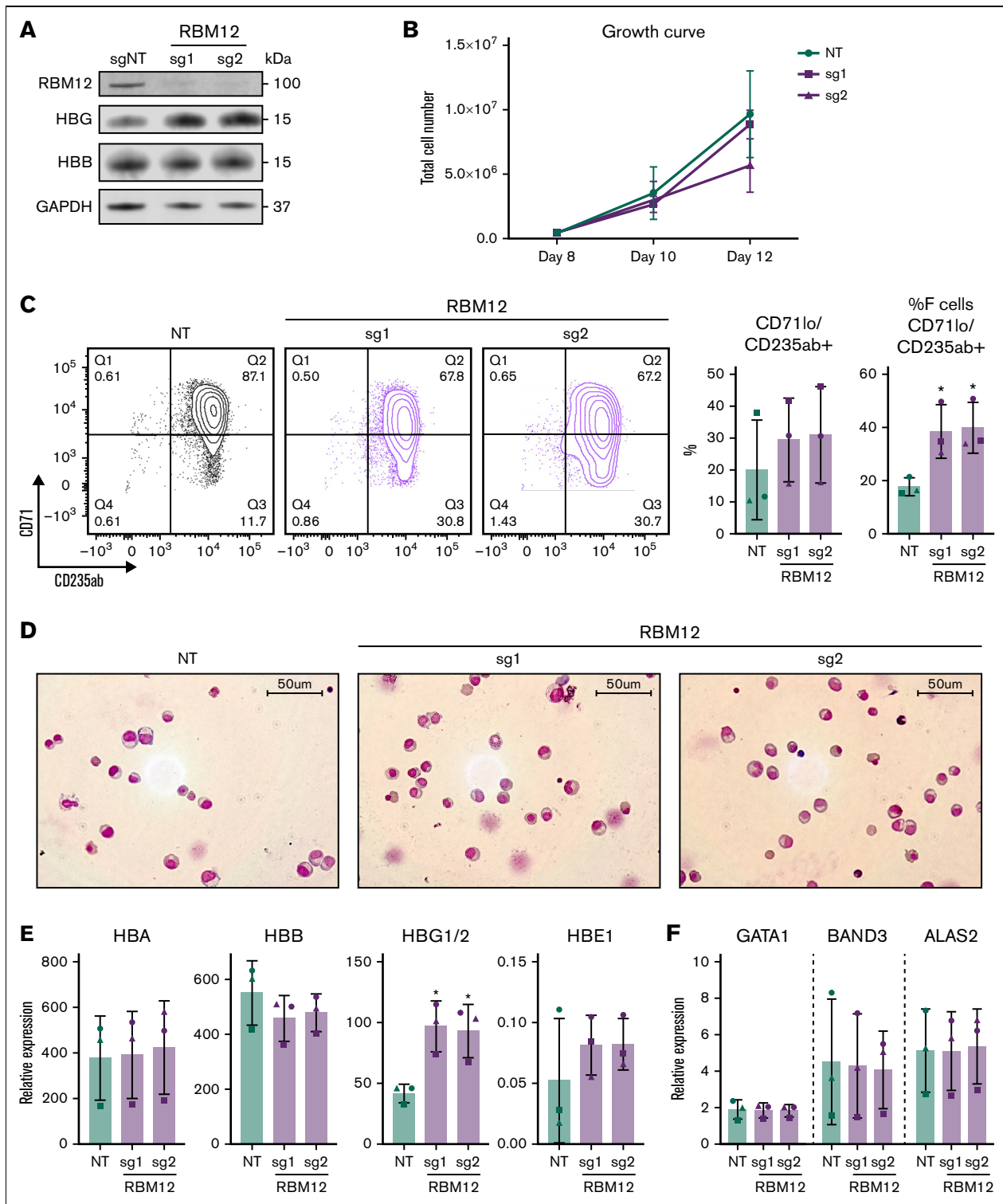
Figure 2. RBM12 depletion in primary human CD34+ HSPCs does not impair erythroid maturation. CRISPR/Cas9 depletion of RBM12 in human CD34+ HSPCs via 2 independent sgRNAs (n = 3 biological replicates). (B, C, E, and F) Plotted are means ± standard deviation. (A) Western blot analysis with indicated antibodies at day 15 of differentiation. (B) Growth curve displaying total cell number from day 8 to 12 of differentiation. (C) Left: Representative contour plots of CD71 vs CD235ab at day 15 of differentiation. Right: Quantification of $CD71_{lo}CD235ab^+$ and $CD71_{lo}CD235ab^+/HbF^+$ cells. *$P < .05$ by Student's t test. (D) Representative May-Grünwald Giemsa images of HSPCs at day 15 of differentiation. (E) qRT-PCR analysis of globin genes at day 12 of differentiation. Results are normalized to *HPRT1*. *$P < .05$ by Student's t test. (F) qRT-PCR analysis of differentiation markers *GATA1*, *BAND3*, and *ALAS2* at day 12 of differentiation. Results are normalized to *HPRT1*.

Importantly, RBM12 depletion did not significantly compromise cellular maturation (Figure 2). Because of the consistent HbF induction along with maintenance of cellular maturation upon depletion in primary human culture, we focused our efforts on characterizing RBM12 in the context of HbF regulation.

RBM12 characterization

RBM12 (also known as SH3/WW domain anchor protein in the nucleus, *SWAN*) contains 5 RRMs, 2 proline-rich regions, and several putative transmembrane domains.[27] Alternative splicing of *RBM12* results in 4 isoforms, all sharing the same coding sequence.[28] Increased *RBM12* expression has been correlated with poor prognosis in hepatocellular and Meibomian cell carcinoma,[29,30] and various mutations in *RBM12* have been found to be associated with endometrial and colorectal cancer diagnoses.[31,32] Additionally, truncating mutations in *RBM12* have been reported in a cohort of patients with psychosis.[33] Despite the various studies citing its potential role in cancer and neurological disorders, there are no studies characterizing its molecular function to date.

The roles of RBPs can be narrowed down by assessing their nuclear localization.[34] We carried out anti-RBM12 immunofluorescence staining in primary human erythroblasts and HeLa cells and found that RBM12 displayed nuclear localization (supplemental Figure 3A), suggesting that it functions at the level of pre-mRNA synthesis or processing. Available tissue-expression databases display expression across various tissue types, including the hematopoietic system (supplemental Figure 3B).[35] In the erythroid compartment, *RBM12* levels are initially high, but fade during terminal differentiation (supplemental Figure 3C-D).[36,37] To assess whether *RBM12* expression is different between fetal and adult stages, as is the case for several developmental globin regulators,[18,19,38,39] we analyzed published data sets and found its expression to not be developmentally selective (supplemental Figure 3E).[38,40] In sum, RBM12 is a nuclear RBP with broad tissue expression that remains unchanged between fetal and adult erythroid stages.

RBM12 influences developmental control of β-globin genes in mice

Human and mouse orthologs of RBM12 share 86.4% amino acid identity, with the highest regions of conservation at the 5 RRMs (supplemental Figure 4A). To test whether RBM12 activity is conserved across mammals, we depleted it via retroviral delivery of sgRNAs into embryonic day 14.5 murine fetal liver erythroblasts (representing adult erythroid cells) expressing Cas9 (supplemental Figure 4B). Unlike humans, mice do not express a fetal form of β-globin, but express 2 embryonic genes, *Hbb-y* and *Hbb-bh1*, both of which also undergo a developmental switch that is controlled by BCL11A and ZBTB7A/LRF, among other factors.[6,41] Upon Rbm12 depletion, transcript levels of *Hbb-bh1*, but not *Hbb-y*, increased (supplemental Figure 4C-D), reminiscent of the increase of *HBG1/2* mRNA but not *HBE1* mRNA in primary human HSPCs upon RBM12 loss (Figure 2E). Additionally, in line with results obtained in human cells, Rbm12 depletion did not delay erythroid maturation, as shown by the normal activation of adult α- and β-globin genes *Hba* and *Hbb-b1* and the repression of the *Kit* gene (supplemental Figure 4E). In sum, RBM12 modulates *Hbb-bh1* levels in murine primary erythroid cells, suggesting that its regulatory influence on the β-globin genes is conserved.

RBM12 depletion increases HbF levels and reduces cell sickling in erythroid cells from patients with SCD

Increased levels of HbF can diminish the propensity of sickle hemoglobin to polymerize under hypoxic conditions and thus inhibit the pathognomonic changes in cell shape.[1,42] To assess whether RBM12 depletion can increase HbF levels sufficient to exert anti-sickling effects, we measured cell sickling in RBM12-depleted erythroid cells in SCD patient–derived CD34^{+} HSPCs upon exposure to 2.5% O_2 for 2 hours. Consistent with results from healthy donors, RBM12 loss triggered a >2-fold increase in *HBG1/2* mRNA and percentage of HbF protein (Figure 3A-B). As a result, we observed a ~50% decrease in cell sickling in the RBM12-depleted samples relative to control (Figure 3C). Together, these results suggest that RBM12 depletion induces HbF to levels sufficient to attenuate cell sickling.

Effects of RBM12 depletion on the erythroid transcriptome and proteome

We next assessed the global impact of RBM12 depletion on the erythroid transcriptome. We performed next-generation sequencing on polyA-selected mRNA (RNA-seq) of primary human erythroblasts from 3 healthy donors following CRISPR/Cas9-mediated depletion of RBM12 (supplemental Figure 5A). Principal component analysis (PCA) revealed clustering of samples from the same donors regardless of RBM12 status, suggesting that RBM12 depletion does not cause widespread changes in the erythroid transcriptome (Figure 4A). Differential gene expression analysis identified 366 upregulated and 301 downregulated genes (fold change >1.5, adjusted $P < 0.05$; Figure 4B). Gene set enrichment analysis against various gene sets available on the Molecular Signatures Database[43,44] found that downregulated transcripts were strongly enriched for interferon-γ and -α response signatures (supplemental Figure 5C). Gene set enrichment analysis against additional gene sets, such as those curated from a variety of sources (including online pathway databases and the literature), also showed enrichment of immune system related pathways among the downregulated genes (supplemental Table 1).

Many nuclear RRM-containing RBPs regulate alternative splicing. Therefore, we analyzed our RNA-seq data for differential splicing using Modeling by Alternative Junction Inclusion Quantification software.[45] Differentially spliced genes (DSGs) were identified as transcripts that contained ≥1 local splicing variation with a >15% difference in inclusion (delta percent spliced in >0.15) of alternative junctions observed between the RBM12-knockout (KO) and NT control conditions. Upon RBM12 depletion, we detected 127 DSGs that contained 133 splicing events. Many of these events that occur upon RBM12 KO included alternative first and last exon splicing and intron retention (Figure 4C).

We next probed changes in the erythroid proteome upon RBM12 depletion. We analyzed nuclear and cytoplasmic extracts from the same set of samples used in RNA-seq by liquid chromatography/tandem mass spectrometry (LC-MS/MS). Samples showed a high degree of correlation with PCA separating samples based on the subcellular origin (supplemental Figure 5D-E). Of the 6620 proteins detected, only 18 were found to be significantly up- or down-regulated in the cytoplasmic fraction (q-value <0.1; Figure 4D; supplemental Table 2). No statistically significant changes were
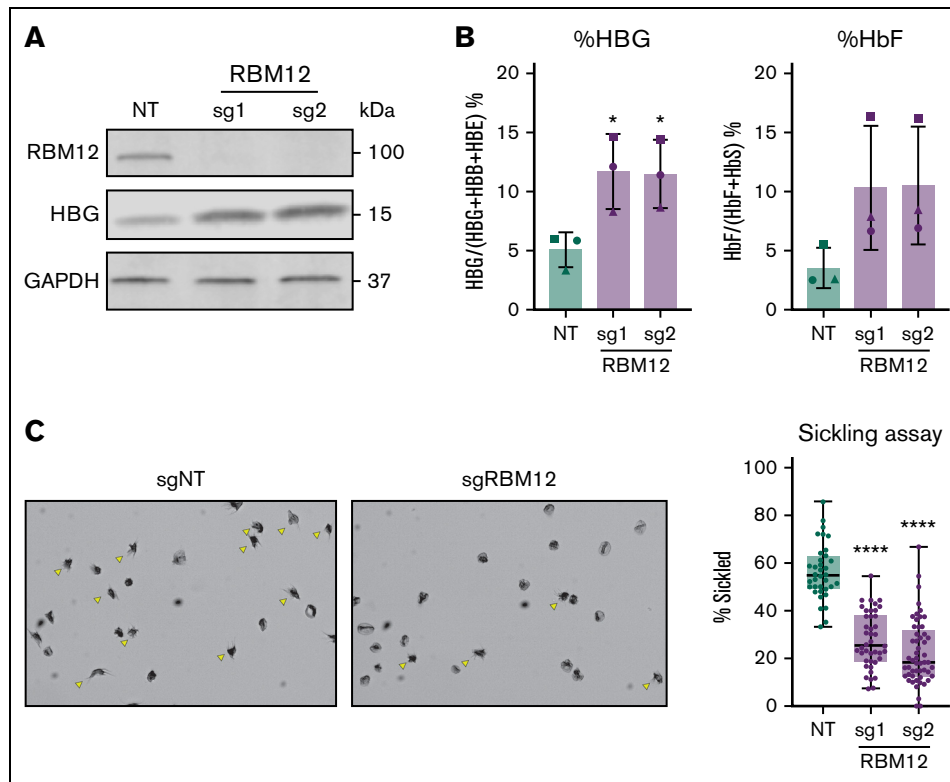
Figure 3. RBM12 depletion in CD34+ HSPCs derived from patients with SCD. CD34+ HSPCs isolated from apheresis waste product of 3 patients with SCD targeted with 2 independent *RBM12* sgRNAs along with an NT control. (A) Western blot analysis with indicated antibodies at day 10 of differentiation. (B) HbF induction assayed via qRT-PCR and high-performance liquid chromatography. Plotted are means ± standard deviation (n = 3). *P < .05 by Student's t test. Left: qRT-PCR of *HBG1/2* mRNA as percentage of total β-like globin transcripts at day 12 of differentiation. Results are normalized to *HPRT1*. Right: High-performance liquid chromatography at day 15 of differentiation. (C) Left: Representative images of sickling assay results. Sickled cells are indicated by yellow arrows. Original magnification ×40 on an Olympus BX40 microscope fitted with an Infinity Lite B camera (Olympus) and the coupled image capture software. Right: Quantification of percent sickled cells. Each dot represents a distinct field of view. Each sample has approximately 1000 total cells quantified. ****P < .0001 by Student's t test.

detected in the nuclear fraction (data not shown). Several of the proteins that were differentially expressed have been linked to cancer prognosis,[46,47] which is in line with previous reports of RBM12's association with various cancers. Additionally, proteins implicated in innate immune system regulation, such as DDX60 and IFI35, were significantly downregulated,[48,49] providing a link to the downregulated immune signatures identified at the transcript level.

Intersecting the RNA-seq and LC-MS/MS data to identify changes commonly found in both datasets, we specifically looked at the expression of the RBP candidates from the CRISPR/Cas9 screen, erythroid transcription factors, globin chains, and known HbF regulators (Figure 4E and supplemental Figure 5F).[50] As expected, HBG1/2 was upregulated in mRNA and protein abundance. HBZ, which encodes for the embryonic α-globin chain, was also found to be upregulated, albeit at low baseline expression. We note that, even though HBG1/2 and HBZ upregulation were found to be statistically significant in transcript abundance, they did not reach the q-value cutoff in protein abundance. We found that RBM12 depletion does not alter the expression of major known HbF regulators and cofactors, suggesting that it functions via a novel pathway. This was individually confirmed via Western blotting and qRT-PCR for BCL11A and ZBTB7A/LRF (supplemental Figure 5G).

In sum, RBM12 reduction in primary human HSPCs does not cause large changes in the erythroid transcriptome or proteome, in line with the observation that RBM12 loss seems to be of little consequence to erythroid fitness and maturation. Furthermore, the lack of changes in known HbF regulators implicates a pathway that does not involve altering the expression of major known HbF repressors and their coregulators.

RBM12 preferentially binds mRNA at the 5'UTR

The position of RBPs on their target RNAs might inform their function.[51] To probe the molecular function of RBM12, we queried its binding pattern via eCLIP-seq.[22] After reproducing a published PTBP1 eCLIP-seq experiment in K562 cells as a technical pilot (supplemental Figure 6), we assayed RBM12 binding in WT primary human erythroblasts. We obtained a total of 1358 high-confidence RBM12-bound peaks at 680 transcripts. Many of the transcripts bound were protein coding genes, followed by long noncoding RNAs (Figure 5A). Interestingly, RBM12-bound peaks were enriched at the 5′UTR (Figure 5B). Gene Ontology analysis revealed that a majority of these 5′UTR-bound transcripts play a role in a variety of transcriptional and posttranscriptional functions (Figure 5C). Intersection with the RNA-seq data revealed that levels of transcripts bound by RBM12 at the 5′UTR, and in general,
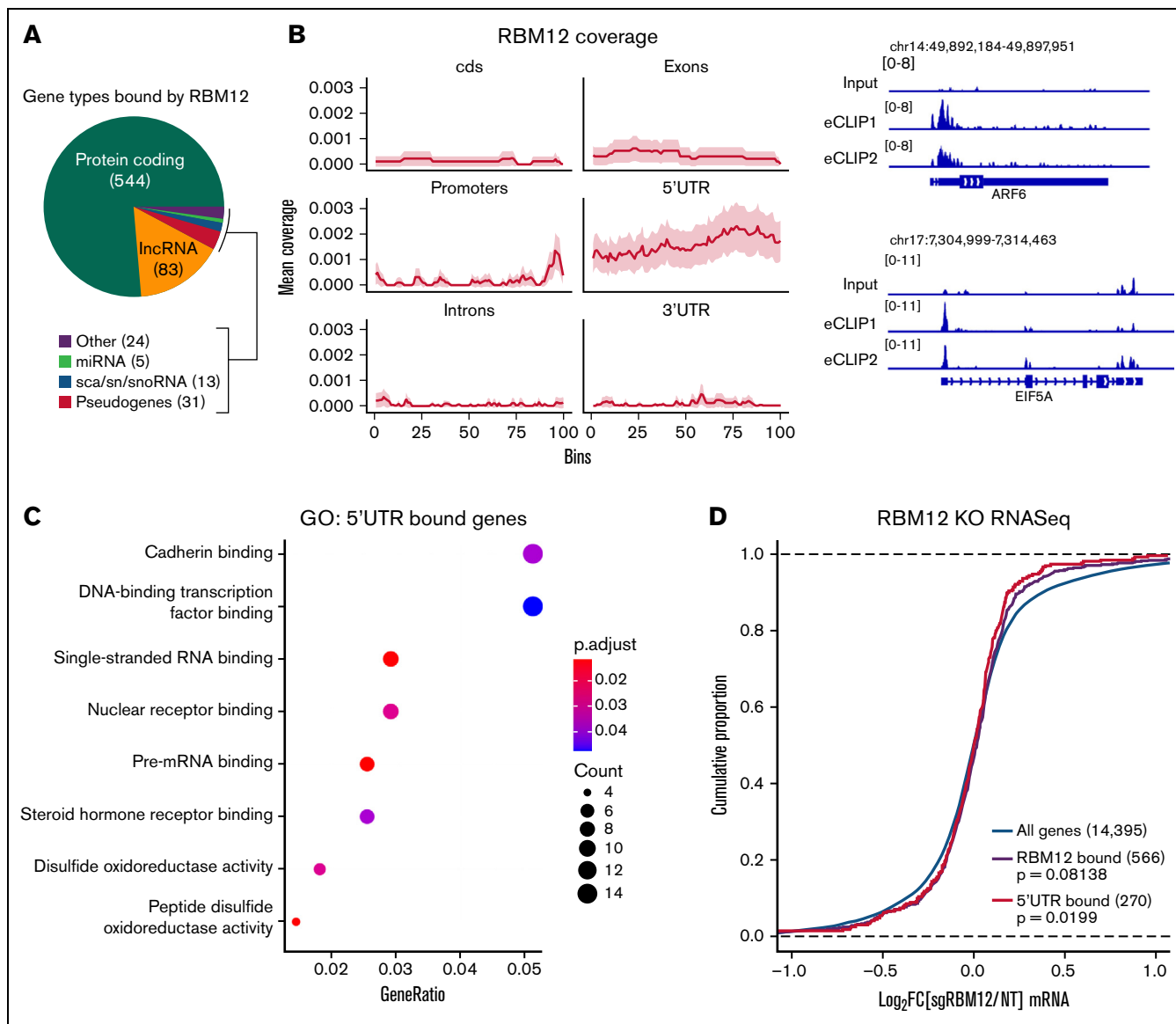
Figure 4. Effects of RBM12 depletion on transcriptome and proteome. (A) PCA of normalized read counts from RBM12-knockout (KO) RNA-seq in primary human erythroblasts at day 7 of differentiation. (B) Volcano plot of differentially expressed transcripts. Highlighted are transcripts found to be differentially expressed with a fold change ≥1.5 and adjusted $P < 0.05$. (C) Pie chart displaying abundance of alternative splicing events occurring among differentially spliced genes (DSGs). (D) Volcano plot of the cytoplasmic fraction of RBM12-KO liquid chromatography/tandem mass spectrometry in primary human erythroblasts at day 7 of differentiation. Highlighted and labeled are proteins found to be differentially expressed with a q-value <0.1. (E) Transcripts per million (TPM; top) and fold change protein abundance (bottom) of RBM12 KO vs NT control samples (n = 3 independent donors).

Figure 5. RBM12 binding patterns. RBM12 eCLIP-seq in WT primary human erythroblasts at day 8 of differentiation. (A) Pie chart displaying the distribution of gene types bound by RBM12. (B) Left: Coverage profile of RBM12 binding. Each feature was divided into 100 bins of equal length. Right: Representative Integrative Genomics Viewer snapshots of RBM12-bound genes. Displayed are the size-matched input control and 2 replicate eCLIP tracks. (C) Gene Ontology (GO) analysis of transcripts bound at the 5′UTR by RBM12. (D) Empirical cumulative distribution function plot displaying log2 fold change in transcript abundance of RBM12 KO samples over control along with RBM12 bound peaks (in general and specifically at 5′UTR). *P* values calculated by Kolmogorov-Smirnoff test.

were unchanged following RBM12 depletion (Figure 5D). Based on these results, RBM12 displays preferential binding at the 5′UTR of its target mRNAs in primary human erythroblasts. The transcripts that are bound by RBM12 are also unchanged at the transcriptional level, indicating a mechanism that likely does not converge on mature transcript abundance.

Mechanistic insight into RBM12 mediated HbF regulation

Although RBM12 depletion was well tolerated in primary human erythroblasts, we were unable to derive homozygous *RBM12* KO clonal HUDEP2 cell lines. Even haploinsufficient *RBM12* HUDEP2

cells (*RBM12*^{+/−}) grew slower than their parental counterparts (supplemental Figure 7A-B). Nevertheless, *RBM12*^{+/−} cells did exhibit increased HbF levels relative to WT, and restoration via expression of full-length *RBM12* (*RBM12*-FL) rescued its HbF-repressive function (supplemental Figure 7C-D).

We used the *RBM12*^{+/−} clones to rule out a potential confounder. *RBM12* shares its promoter with another gene, *CPNE1*. Genes that share promoters are often coregulated,[28] and, in line with this observation, we found that *CPNE1* expression is strongly correlated with *RBM12* expression, as its expression is depleted in *RBM12*^{+/−} clones and is restored upon *RBM12*-FL overexpression (supplemental Figure 8A-B). Therefore, we
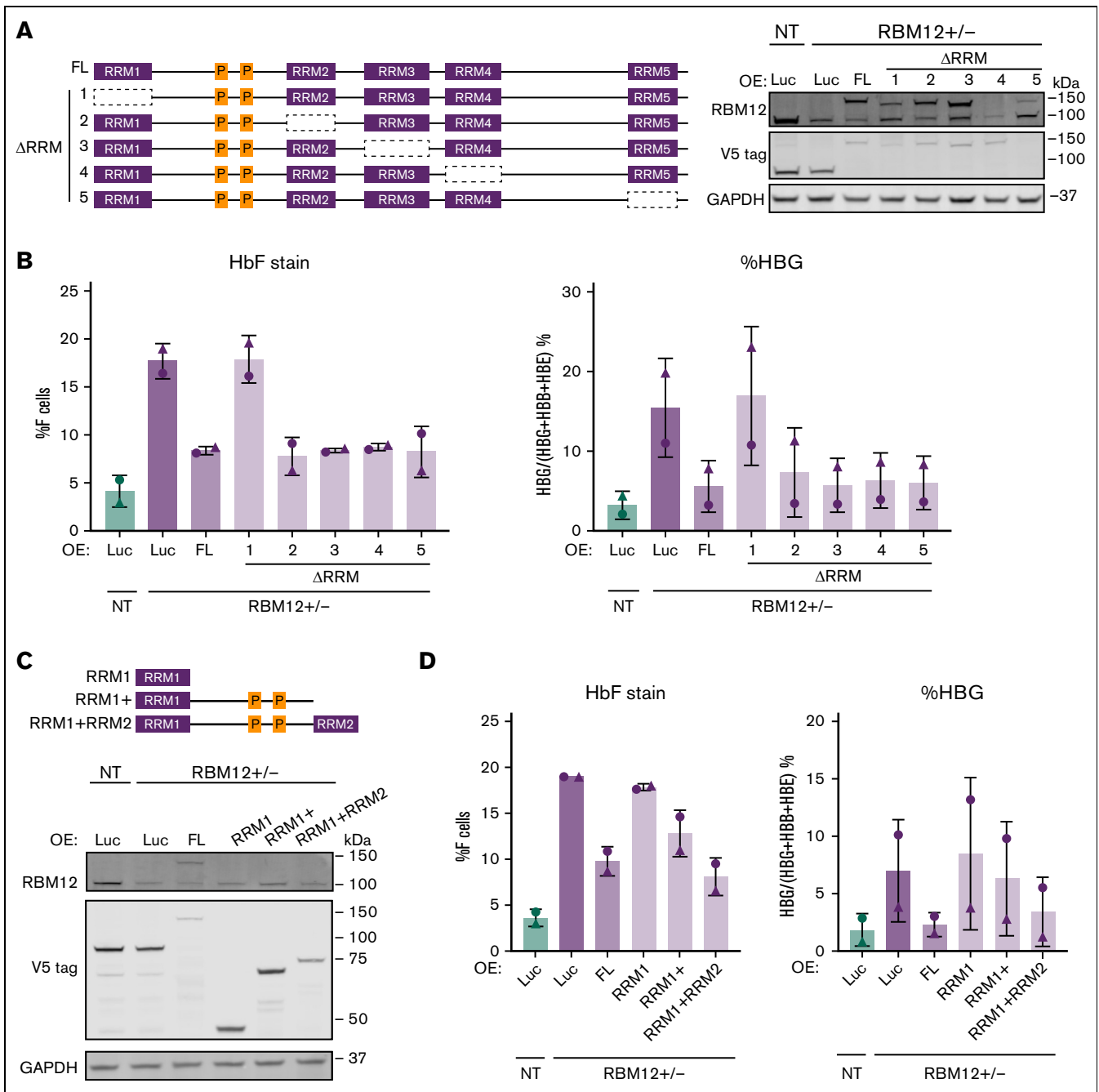
Figure 6. Structure function analysis of RBM12 RRM domains. Two independent RBM12^{+/−} clones were infected with lentivirus containing conditional *RBM12* overexpression (OE) and luciferase control constructs. (B and D) Plotted are means ± standard deviation. (A) Left: Schematic of various forms of *RBM12* OE constructs. Right: Representative Western blot of mutant *RBM12* OE constructs with indicated antibodies. (B) HbF flow cytometry (left) and qRT-PCR of *HBG1/2* mRNA as percentage of total β-like globin transcripts (right) at day 5 of differentiation. (C) Top: Schematic of RBM12 truncated OE constructs. Bottom: Representative Western blot of *RBM12* truncated OE constructs with indicated antibodies. (D) HbF flow cytometry (left) and qRT-PCR of *HBG1/2* mRNA as percentage of total β-like globin transcripts (right) at day 5 of differentiation.

tested CPNE1's ability as the true HbF repressor behind RBM12 depletion by overexpressing *CPNE1* in *RBM12^{+/−}* clones. We found that this was not the case, as CPNE1 failed to rescue HbF repression (supplemental Figure 8C-D). Thus, we can conclude that the altered HbF levels are truly RBM12-mediated.

We next asked which of the 5 RRM domains are important for RBM12's function in HbF repression. The existence of multiple RRMs in RBPs allows for increased affinity and specificity in binding mRNA targets.[52] We overexpressed in 2 independent *RBM12^{+/−}* clones, *RBM12*-FL and mutants lacking one of each RRM (ΔRRM1-5), and measured HbF induction (Figure 6A). Luciferase

overexpression served as negative control. *RBM12*-FL and every ΔRRM mutant except ΔRRM1 were able to silence HbF expression (Figure 6B). We next tested whether this RRM1 domain is sufficient to repress HbF by overexpressing various truncated forms of RBM12 (Figure 6C). The RRM1 domain alone was insufficient to repress HbF expression; however, the addition of the linker region between RRM1 and RRM2 to RRM1 restored RBM12's HbF-repressive activity (Figure 6D). This linker region contains 2 proline-rich regions, which have been implicated in protein-protein interactions.[53,54] Taken together, the RRM1 domain of RBM12 is necessary for HbF repression and, with the addition of the proline-rich linker region, is sufficient for RBM12-mediated HbF repression. These results suggest that RBM12-mediated HbF regulation likely requires interaction with auxiliary proteins.

Discussion

We performed an RBP-targeted CRISPR/Cas9-based screen in HUDEP2 cells and identified RBM12 as a novel regulator of HbF expression. The degree of HbF induction upon RBM12 loss was sufficient to attenuate cell sickling in SCD-derived erythroid cells. Rbm12 loss in primary murine erythroid cells triggered derepression of embryonic β-type globin genes, suggesting conserved function across mammals. RBM12 depletion displayed minimal alterations to the erythroid transcriptome and proteome, consistent with an ostensible lack of detrimental effects to erythroid maturation. Additionally, differential splicing analysis yielded an abundance of intron retention and alternative first- and last-exon splicing events. Mechanistically, the HbF-silencing activity of RBM12 can be reduced to a single RRM domain plus a proline-rich linker region. eCLIP-seq demonstrates that RBM12 preferentially binds 5′UTRs of mRNA transcripts, providing a hint into its molecular function.

HUDEP2 cells present a powerful screening tool in which, historically, most hits have been validated in parallel cell systems.[21,55] In this case, among 4 hits, only the loss of RBM12 produced significant HbF induction in primary cultured erythroid cells in the absence of detrimental effects to cell maturation. Although this discrepancy between systems is not sufficient to rule out the other 3 proteins as HbF regulators, it does highlight potential limitations of the in vitro cell systems used. *SYNCRIP*, *hnRNPM*, and *PTBP1* belong to a group of RBPs known as heterogeneous nuclear ribonucleoproteins (hnRNPs).[17] Interestingly, these hnRNPs have been reported to regulate the alternative splicing of each other's transcripts.[56] Studying the potential cooperative effects among these hnRNPs might confirm or rule out any role in HbF regulation. Because RBM12 was validated in both cell systems, follow-up studies focused on this protein.

To explore the molecular mechanisms by which RBM12 regulates HbF levels, we characterized the subcellular localization of RBM12, assessed the transcriptome and proteome of RBM12-depleted cells, and interrogated its RNA binding profiles. This led to the following insights: first, RBM12 is localized to the nucleus, making a direct role in mRNA translation or stability unlikely, favoring a role in pre-mRNA synthesis or processing. The majority of the 680 mRNAs bound by RBM12 lack corresponding changes in protein levels and are also not differentially spliced (supplemental Figure 7). In the case of mRNAs bound that do overlap with DSGs, the RBM12 eCLIP-seq peaks do not overlap with the splice junction coordinates. Hence, simple binding to mRNA by RBM12 might not be sufficient to effect measurable changes in mRNA processing. Second, eCLIP-seq analysis revealed that RBM12 preferentially binds mRNA in a specific manner, particularly at the 5′UTR. This pattern has previously been reported to occur among select nuclear RBPs such as *NCBP2/CBP20*, a subunit of the cap binding complex.[51] In the nucleus, the cap binding complex plays a role in nuclear export, pre-mRNA processing, and transcriptional regulation.[57,58] Involvement in mRNA nuclear export might be expected to ultimately impinge on mRNA translation. This remains a distinct possibility because our mass spectrometry analysis failed to capture all cellular proteins. Additionally, there remains the possibility that RBM12 plays a role in transcription initiation. Other proteins that are associated with the 5′UTR of nascent mRNA regulate transcription via RNA polymerase II (*RNAPII*) promoter proximal pausing, such as negative elongation factor (*NELF*), which contains subunits that bind RNA.[59,60] It is therefore possible that, like *NELF*, RBM12 plays a role in regulation of RNAPII pause-release.[61,62] Attempts to detect RBM12 by ChIP at 5′ ends of active genes have failed, which argues against but does not rule out a role in transcription initiation or pause-release.

Because BCL11A and ZBTB7A/LRF are the major repressors of HbF expression, there is a high chance that a putative HbF repression pathway converges on these transcription factors and their coregulators. We found that RBM12 does not measurably impact the levels of either regulator or their cofactors, suggesting that it functions in yet to be discovered pathways or that it post-transcriptionally controls subunits of these protein complexes that were not detected by mass spectrometry. Hence, the pathway by which RBM12 selectively impacts fetal genes remains elusive.

Last, our structure-function analysis of RBM12 not only validated the HbF-regulatory role of RBM12, but also identified the region necessary to carry out HbF modulatory functions, providing additional insight into the role of this undercharacterized RBP. Although the RRM1 region is necessary for HbF repression, the truncated form that includes RRM1 and 2 proline-rich regions displayed sufficiency. The fact that the HbF regulatory function can be reduced to a relatively small portion of the molecule might facilitate means to perturb this function without interfering with other RBM12 functions. It is noteworthy that targeting RBPs via small molecules is an avenue that is currently being explored via disrupting the RNA binding domain and perturbing interactions with target transcripts.[63,64] In the case of RBM12, the RRM1 domain might be a candidate for small molecule inhibitor development to induce HbF expression. However, its broad expression pattern will require further investigation into its suitability as a drug target.

In summary, we identified RBM12 as a novel HbF repressor in human erythroid cells. In addition to the discovery of a potential therapeutic target, we provide the first functional characterization of RBM12. The insights into RBM12 hold promise in the field of erythroid biology by highlighting an undercharacterized branch of HbF regulation.

Acknowledgments

Authorship

Contribution: A.W. and G.A.B. conceived the study, designed the experiments, and wrote the manuscript; A.W., M.Q.-V., C.A.K., B.M.G., R.C.H., and J.S. analyzed the data; A.W., M.K., M.S., A.J.T., M.S.S., O.A., S.A.P., and E.K. performed experiments; and all authors provided input on the manuscript.

Conflict-of-interest disclosure: The authors declare no competing financial interests.

ORCID profiles: M.K., 0000-0002-6258-0069; A.J.T., 0000-0003-1371-7361; M.Q.-V., 0000-0001-9945-8123; O.A., 0000-0003-2497-4291; E.K., 0000-0003-2313-9710; C.A.K., 0000-0001-6594-0245; B.M.G., 0000-0002-4681-1074; Y.B., 0000-0003-3005-5048; R.C.H., 0000-0003-4084-7516; J.S., 0000-0002-8427-6316.

Correspondence: Gerd A. Blobel, Department of Hematology, The Children's Hospital of Philadelphia, 316H Abramson Research Center, 3615 Civic Center Blvd, Philadelphia, PA 19104; email: blobel@e-mail.chop.edu.

References

1. Wienert B, Martyn GE, Funnell APW, Quinlan KGR, Crossley M. Wake-up sleepy gene: reactivating fetal globin for β-hemoglobinopathies. *Trends Genet*. 2018;34(12):927-940.

2. Sankaran VG, Orkin SH. The switch from fetal to adult hemoglobin. *Cold Spring Harb Perspect Med*. 2013;3(1):a011643.

3. Platt OS, Brambilla DJ, Rosse WF, et al. Mortality in sickle cell disease. Life expectancy and risk factors for early death. *N Engl J Med*. 1994;330(23):1639-1644.

4. Martyn GE, Wienert B, Yang L, et al. Natural regulatory mutations elevate the fetal globin gene via disruption of BCL11A or ZBTB7A binding. *Nat Genet*. 2018;50(4):498-503.

5. Liu N, Hargreaves VV, Zhu Q, et al. Direct promoter repression by BCL11A controls the fetal to adult hemoglobin switch. *Cell*. 2018;173(2):430-442.e17.

6. Masuda T, Wang X, Maeda M, et al. Transcription factors LRF and BCL11A independently repress expression of fetal hemoglobin. *Science*. 2016;351(6270):285-289.

7. Lan X, Ren R, Feng R, et al. ZNF410 uniquely activates the NuRD component CHD4 to silence fetal hemoglobin expression. *Mol Cell*. 2021;81(2):239-254.e8.

8. Vinjamur DS, Yao Q, Cole MA, et al. ZNF410 represses fetal globin by singular control of CHD4. *Nat Genet*. 2021;53(5):719-728.

9. Huang P, Peslak SA, Lan X, et al. The HRI-regulated transcription factor ATF4 activates BCL11A transcription to silence fetal hemoglobin expression. *Blood*. 2020;135(24):2121-2132.

10. Basak A, Munschauer M, Lareau CA, et al. Control of human hemoglobin switching by LIN28B-mediated regulation of BCL11A translation. *Nat Genet*. 2020;52(2):138-145.

11. de Rooij LPMH, Chan DCH, Keyvani Chahi A, Hope KJ. Post-transcriptional regulation in hematopoiesis: RNA binding proteins take control. *Biochem Cell Biol*. 2019;97(1):10-20.

12. Paralkar VR, Weiss MJ. Long noncoding RNAs in biology and hematopoiesis. *Blood*. 2013;121(24):4842-4846.

13. Khajuria RK, Munschauer M, Ulirsch JC, et al. Ribosome levels selectively regulate translation and lineage commitment in human hematopoiesis. *Cell*. 2018;173(1):90-103.e19.

14. Edwards CR, Middleton R, An X, et al. A dynamic intron retention program in the mammalian megakaryocyte and erythrocyte lineages. *Blood*. 2015;126(23):2380.

15. Pimentel H, Parra M, Gee SL, Mohandas N, Pachter L, Conboy JG. A dynamic intron retention program enriched in RNA processing genes regulates gene expression during terminal erythropoiesis. *Nucleic Acids Res*. 2016;44(2):838-851.

16. Chakalova L, Osborne CS, Dai Y-F, et al. The Corfu thalassemia deletion disrupts-globin gene silencing and reveals post-transcriptional regulation of HbF expression. *Blood*. 2005;105(5):2154-2160.

17. Dreyfuss G, Kim VN, Kataoka N. Messenger-RNA-binding proteins and the messages they carry. *Nat Rev Mol Cell Biol*. 2002;3(3):195-205.

18. Lee YT, de Vasconcellos JF, Yuan J, et al. LIN28B-mediated expression of fetal hemoglobin and production of fetal-like erythrocytes from adult human erythroblasts ex vivo. *Blood*. 2013;122(6):1034-1041.

19. de Vasconcellos JF, Tumburu L, Byrnes C, et al. IGF2BP1 overexpression causes fetal-like hemoglobin expression patterns in cultured human adult erythroblasts. *Proc Natl Acad Sci USA*. 2017;114(28):E5664-E5672.

20. Shi J, Wang E, Milazzo JP, Wang Z, Kinney JB, Vakoc CR. Discovery of cancer drug targets by CRISPR-Cas9 screening of protein domains. *Nat Biotechnol*. 2015;33(6):661-667.

21. Grevet JD, Lan X, Hamagami N, et al. Domain-focused CRISPR screen identifies HRI as a fetal hemoglobin regulator in human erythroid cells. *Science*. 2018;361(6399):285-290.

22. Van Nostrand EL, Pratt GA, Shishkin AA, et al. Robust transcriptome-wide discovery of RNA-binding protein binding sites with enhanced CLIP (eCLIP). *Nat Methods*. 2016;13(6):508-514.

23. Littlewood TD, Hancock DC, Danielian PS, Parker MG, Evan GI. A modified oestrogen receptor ligand-binding domain as an improved switch for the regulation of heterologous proteins. *Nucleic Acids Res*. 1995;23(10):1686-1690.

24. Maris C, Dominguez C, Allain FH-T. The RNA recognition motif, a plastic RNA-binding platform to regulate post-transcriptional gene expression. *FEBS J*. 2005;272(9):2118-2131.

25. Hu J, Liu J, Xue F, et al. Isolation and functional characterization of human erythroblasts at distinct stages: implications for understanding of normal and disordered erythropoiesis in vivo. *Blood*. 2013;121(16):3246-3253.

26. Brinkman EK, Chen T, Amendola M, van Steensel B. Easy quantitative assessment of genome editing by sequence trace decomposition. Nucleic Acids Res. 2014 Dec 16;42(22):e168. https://doi.org/10.1093/nar/gku936

27. Stover C, Gradl G, Jentsch I, Speicher MR, Wieser R, Schwaeble W. cDNA cloning, chromosome assignment, and genomic structure of a human gene encoding a novel member of the RBM family. *Cytogenet Cell Genet*. 2001;92(3-4):225-230.

28. Yang W, Ng P, Zhao M, Wong TK, Yiu SM, Lau YL. Promoter-sharing by different genes in human genome–CPNE1 and RBM12 gene pair as an example. *BMC Genomics*. 2008;9(1):456.

29. Gao C, Shen J, Chen W, et al. Increased *RBM12* expression predicts poor prognosis in hepatocellular carcinoma based on bioinformatics. *J Gastrointest Oncol*. 2021;12(4):1905-1926.

30. Kumar A, Kumar Dorairaj S, Prabhakaran VC, Prakash DR, Chakraborty S. Identification of genes associated with tumorigenesis of meibomian cell carcinoma by microarray analysis. *Genomics*. 2007;90(5):559-566.

31. Shivakumar M, Miller JE, Dasari VR, Gogoi R, Kim D. Exome-wide rare variant analysis from the discovehr study identifies novel candidate predisposition genes for endometrial cancer. *Front Oncol*. 2019;9:574.

32. Giannakis M, Mu XJ, Shukla SA, et al. Genomic correlates of immune-cell infiltrates in colorectal carcinoma. *Cell Rep*. 2016;15(4):857-865.

33. Steinberg S, Gudmundsdottir S, Sveinbjornsson G, et al. Truncating mutations in RBM12 are associated with psychosis. *Nat Genet*. 2017;49(8):1251-1254.

34. Gerstberger S, Hafner M, Tuschl T. A census of human RNA-binding proteins. *Nat Rev Genet*. 2014;15(12):829-845.

35. GTEx Consortium. The Genotype-Tissue Expression (GTEx) project. *Nat Genet*. 2013;45(6):580-585.

36. Bagger FO, Kinalis S, Rapin N. BloodSpot: a database of healthy and malignant haematopoiesis updated with purified and single cell mRNA sequencing profiles. *Nucleic Acids Res*. 2019;47(D1):D881-D885.

37. An X, Schulz VP, Li J, et al. Global transcriptome analyses of human and murine terminal erythroid differentiation. *Blood*. 2014;123(22):3466-3477.

38. Huang P, Keller CA, Giardine B, et al. Comparative analysis of three-dimensional chromosomal architecture identifies a novel fetal hemoglobin regulatory element. *Genes Dev*. 2017;31(16):1704-1713.

39. Sankaran VG, Xu J, Ragoczy T, et al. Developmental and species-divergent globin switching are driven by BCL11A. *Nature*. 2009;460(7259):1093-1097.

40. Lessard S, Beaudoin M, Orkin SH, Bauer DE, Lettre G. 14q32 and let-7 microRNAs regulate transcriptional networks in fetal and adult human erythroblasts. *Hum Mol Genet*. 2018;27(8):1411-1420.

41. Kingsley PD, Malik J, Emerson RL, et al. "Maturational" globin switching in primary primitive erythroid cells. *Blood*. 2006;107(4):1665-1672.

42. Rees DC, Williams TN, Gladwin MT. Sickle-cell disease. *Lancet*. 2010;376(9757):2018-2031.

43. Subramanian A, Tamayo P, Mootha VK, et al. Gene set enrichment analysis: a knowledge-based approach for interpreting genome-wide expression profiles. *Proc Natl Acad Sci USA*. 2005;102(43):15545-15550.

44. Liberzon A, Birger C, Thorvaldsdóttir H, Ghandi M, Mesirov JP, Tamayo P. The Molecular Signatures Database (MSigDB) hallmark gene set collection. *Cell Syst*. 2015;1(6):417-425.

45. Vaquero-Garcia J, Barrera A, Gazzara MR, et al. A new view of transcriptome complexity and regulation through the lens of local splicing variations. *eLife*. 2016;5:e11752.

46. Rosenberg EE, Prudnikova TY, Zabarovsky ER, Kashuba VI, Grigorieva EV. D-glucuronyl C5-epimerase cell type specifically affects angiogenesis pathway in different prostate cancer cells. *Tumour Biol*. 2014;35(4):3237-3245.

47. Qin X, Liu Z, Yan K, Fang Z, Fan Y. Integral analysis of the RNA binding protein-associated prognostic model for renal cell carcinoma. *Int J Med Sci*. 2021;18(4):953-963.

48. Oshiumi H, Miyashita M, Okamoto M, et al. DDX60 is involved in RIG-I-dependent and independent antiviral responses, and its function is attenuated by virus-induced EGFR activation. *Cell Rep*. 2015;11(8):1193-1207.

49. De Masi R, Orlando S, Bagordo F, Grassi T. IFP35 is a relevant factor in innate immunity, multiple sclerosis, and other chronic inflammatory diseases: a review. *Biology (Basel)*. 2021;10(12):1325.

50. Sher F, Hossain M, Seruggia D, et al. Rational targeting of a NuRD subcomplex guided by comprehensive in situ mutagenesis. *Nat Genet*. 2019;51(7): 1149-1159.

51. Van Nostrand EL, Pratt GA, Yee BA, et al. Principles of RNA processing from analysis of enhanced CLIP maps for 150 RNA binding proteins. *Genome Biol*. 2020;51(1):1-26.

52. Jankowsky E, Harris ME. Specificity and nonspecificity in RNA-protein interactions. *Nat Rev Mol Cell Biol*. 2015;16(9):533-544.

53. Kurochkina N, Guha U. SH3 domains: modules of protein-protein interactions. *Biophys Rev*. 2013;5(1):29-39.

54. Kay BK, Williamson MP, Sudol M. The importance of being proline: the interaction of proline-rich motifs in signaling proteins with their cognate domains. *FASEB J*. 2000;14(2):231-241.

55. Lan X, Khandros E, Huang P, et al. The E3 ligase adaptor molecule SPOP regulates fetal hemoglobin levels in adult erythroid cells. *Blood Adv*. 2019; 3(10):1586-1597.

56. Huelga SC, Vu AQ, Arnold JD, et al. Integrative genome-wide analysis reveals cooperative regulation of alternative splicing by hnRNP proteins. *Cell Rep*. 2012;1(2):167-178.

57. Rambout X, Maquat LE. The nuclear cap-binding complex as choreographer of gene transcription and pre-mRNA processing. *Genes Dev*. 2020; 34(17-18):1113-1127.

58. Galloway A, Cowling VH. mRNA cap regulation in mammalian cell function and fate. *Biochim Biophys Acta Gene Regul Mech*. 2019;1862(3):270-279.

59. Core L, Adelman K. Promoter-proximal pausing of RNA polymerase II: a nexus of gene regulation. *Genes Dev*. 2019;33(15-16):960-982.

60. Vos SM, Pöllmann D, Caizzi L, et al. Architecture and RNA binding of the human negative elongation factor. *eLife*. 2016;5:e14981.

61. Yamamoto J, Hagiwara Y, Chiba K, et al. DSIF and NELF interact with Integrator to specify the correct post-transcriptional fate of snRNA genes. *Nat Commun*. 2014;5(1):4263.

62. Narita T, Yung TMC, Yamamoto J, et al. NELF interacts with CBC and participates in 3′ end processing of replication-dependent histone mRNAs. *Mol Cell*. 2007;26(3):349-365.

63. Mohibi S, Chen X, Zhang J. Cancer the 'RBP'eutics-RNA-binding proteins as therapeutic targets for cancer. *Pharmacol Ther*. 2019;203:107390.

64. Clingman CC, Deveau LM, Hay SA, et al. Allosteric inhibition of a stem cell RNA-binding protein by an intermediary metabolite. *eLife*. 2014;3:e02848.